



Article

Development and Mechanical Properties of Basalt Fiber-Reinforced Acrylonitrile Butadiene Styrene for In-Space Manufacturing Applications

Natalie Coughlin, Bradley Drake , Mikala Fjerstad, Easton Schuster, Tyler Waege, Adrian Weerakkody and Todd Letcher *

Mechanical Engineering Department, South Dakota State University, Brookings, SD 57007, USA

* Correspondence: todd.letcher@sdstate.edu; Tel.: +1-605-688-5311

Received: 1 July 2019; Accepted: 2 September 2019; Published: 5 September 2019



Abstract: A new basalt fiber reinforced acrylonitrile butadiene styrene (ABS) filament has been developed for fused filament fabrication (FFF, 3D printing) to be used in Mars habitat construction. Building habitats on Mars will be expensive, especially if all material must be shipped from earth. However, if some materials can be used from Mars, costs will dramatically decrease. Basalt is easily mined from the surface of Mars. This study details the production process of the material, experimental results from mechanical testing, and preliminary X-ray shielding characteristics. The addition of chopped 3 mm basalt fibers to standard FFF material, ABS, increased strength and stiffness of the composite material. By adding 25% (by weight) basalt fiber to ABS, tensile strength improved nearly 40% by increasing from 36.55 MPa to 50.58 MPa, while Modulus of Elasticity increased about 120% from 2.15 GPa to 4.79 GPa. Flexural strength increased by about 20% from 56.94 MPa to 68.51 MPa, while Flexural Modulus increased by about 70% from 1.81 GPa to 3.05 GPa. While compression results did not see much strength improvements, the addition of fibers also did not decrease compressive strength. This is important when considering that basalt fibers provide radiation shielding and the cost of adding basalt fibers to construction materials on Mars will be negligible compared to the cost of shipping other materials from earth. In preliminary digital radiography testing, it was shown that 77% of X-rays were shielded with 25% basalt fiber added (as compared to neat ABS). In small-scale 3D printing applications, the 25% fiber ratio seems to be the highest ratio that provides reliable FFF printing.

Keywords: basalt fiber; ABS; 3D printing; additive manufacturing; extruding; high strength filament

1. Introduction

The goal of this paper is to develop a novel material feedstock for in-space manufacturing applications to be used for long duration exploration missions, ideally leading to the ability to 3D print a habitat off-earth. In particular, this paper will focus on developing a material for the construction of habitats on the surface of Mars, as NASA has announced a Mars mission in the near future [1]. An ideal material would be strong, stiff, impact resistant, and provide radiation shielding for the astronauts and equipment inside the habitat. The material should also contain as much locally available (on Mars) materials to minimize the amount of building supplies that need to be shipped to Mars. Most likely, this material will need to be a thermoplastic composite material in order to be easily 3D printed. In the short term, the goal is to develop this material for small-scale 3D printing testing on earth and at the International Space Station (ISS) using the Additive Manufacturing Facility [2].

The off-earth application of this material leads to different ways of thinking about using materials in a composite material design process. Because Mars is far from earth, transporting any cargo from

Earth to Mars will be expensive [3]. Transporting all building materials from Earth to Mars will likely be cost prohibitive. The most reasonable alternative is to use as much locally available material as possible along with any recyclable waste from cargo missions, such as packaging materials. This is different than traditional composite material design, in which there is an optimization between the amount of reinforcing fibrous material that strengthens the material and cost of the fibrous materials. In the application of in-space manufacturing, the cost of the reinforcing material would be negligible because it would be found on the surface of Mars and the cost of the matrix material would be expensive due to shipping costs to Mars. This changes the normal design considerations from traditional decisions made for earth-based applications. However, because this material is expected to be 3D printed on Mars and the ISS, there are some 3D printing considerations that must be accounted for too.

Using fused filament fabrication (FFF), molten thermoplastic (or a thermoplastic with a property enhancing additive) is pushed through a heated nozzle and selectively deposited on a build plate. Obviously, the deposition toolpath will play an important role in the overall strength of the additively manufactured component [4–9]. Many studies have shown that specific printing orientation and toolpaths and even layer thicknesses can create stronger parts in a specific direction. However, this often means sacrificing strength in another direction. Typically, FFF manufactured parts will use alternating toolpath directions on sequential layers to mitigate these effects (similar to some composite materials). The addition of reinforcing fibers to the printed material only increases these effects in FFF parts [10].

For many years, FFF was limited to specific thermoplastic materials. However, in recent years, new material development for FFF has seen an increase in demand and activity. Many of the new materials being developed are composite materials, with the goal of increasing a specific material property. In 2015, the first 3D printable graphene composites were being tested as an acrylonitrile butadiene styrene (ABS) composite material [11]. Other variants of biocompatible graphene composite materials are also being tested [12]. In this case, a blended TPU and PLA matrix material is used along with graphene oxide to tailor properties as required for the application. In other cases, multi-walled carbon nanotubes were paired with an ABS matrix to increase tensile and flexural strength and stiffness and increase the heat deflection temperature [12,13]. Thermal properties of 3D printable materials have also been altered to suit a particular 3D printing application. Boron nitride was added to ABS material to increase the thermal conductivity by about 3–4 times with a boron nitride weight ratio of 40% [14]. The goal of this composite material was to increase thermal conductivity to be able to 3D print a heat dispersive device.

Most of the research in composite material 3D printing is related to a thermoplastic with a fiber reinforcing material [15–20]. Most of these materials have focused on short discontinuous fibers because this is a much simpler and less expensive method for FFF printing. However, some specialized equipment is able to print using long continuous fiber tows embedded into the 3D printed component [21–24]. Most of these studies have focused on small-scale 3D printed components, however, some work has been done to understand large 3D printed composite materials used in the construction industry. The strength of 3D printed geo-polymer mortar reinforced with glass fibers was studied as a sustainable construction method and material [18]. Structures of approximately one cubic meter were able to be constructed and tested, showing that increasing fiber content generally strengthened the material in flexural and compressive loading scenarios.

None of the materials used in any of the previously discussed research are readily available on the surface of Mars. The surface of Mars is similar to parts of the earth's crust. The Mars surface is basically a layer of fine dust particles covering a mostly volcanic basalt rock layer estimated to be 6 to 30 miles thick [25–27]. From these basalt rocks, basalt fibers can be produced using methods similar to the methods used to make glass fibers [28]. Basalt fiber composite materials have been investigated for many applications, including as a replacement fiber to asbestos applications [29,30]. Several studies have been conducted on the use of basalt fiber as a reinforcing material in a thermoplastic composite material [31–36]. Only three studies have focused on 3D printing basalt fiber composite materials and all have used PLA as the matrix material [37–39]. While all of these studies have shown success in

using basalt fibers as a reinforcing material for their specific applications, none have focused on use for in-space manufacturing and the unique design thought process needed for this application.

In the last decade, the concept of using 3D printing for in-space manufacturing has shown great promise towards creating a safe, reliable, and less expensive way of doing business in space [40–43]. In general, the ability to start with raw materials and create components on an as-needed basis greatly reduces the cost and increases the safety of missions. Cost is reduced by not having to ship multiple spare parts when spare parts are not always needed. Mission safety is increased because spare parts can be made as necessary, even if spare parts have not been shipped to the off-earth location. To ensure that 3D printers and 3D printed materials behave as expected in microgravity environments, several studies have been conducted at the ISS [44–47]. Test samples were printed at the ISS and samples were sent back to earth for further testing. These tests proved to be successful and a 3D printer has been permanently installed at the ISS for both emergency part creation and for general component production at the ISS for on-going experiments. In addition to studying small FFF 3D printing, significant research has been conducted in the area of using in-situ materials to create large construction projects off-earth [48–53].

The goal of this paper is to develop a new material that will be strong and stiff and could be used to build a full-size habitat for astronauts to live and work inside. Additionally, radiation is a big concern for astronauts and radiation protection systems must be used. The construction materials being used to create the habitat, should also provide for some radiation protection to minimize astronaut exposure whenever inside the habitat. Last, and most important, this material must use as much material as possible from the surface of Mars because shipping materials to Mars will be expensive. The rest of the paper will detail the material development process and the reasons that led to the study of a basalt reinforced ABS composite material, and provide experimental test data for critical material properties for this application.

2. Materials and Methods

In this study, a new ABS-Basalt fiber composite material is developed and tested using a fused filament fabrication (FFF) method of manufacturing final parts. The material preparation process (detailed in later sections) results in a 1.75 mm filament, which is then used in an FFF 3D printer to manufacture test samples. Several ratios of basalt fiber to ABS matrix of this material were manufactured and tested to determine material properties at each material ratio. In total, 5 material ratios were fabricated (0%, 10%, 25%, 40%, 60% fiber by weight), with 4 of these ratios ultimately being able to be 3D printed. Material property testing included mechanical destructive testing (tensile, flexural, compressive, and impact), microscopic imaging to determine fiber mixing and adherence to the polymer, and X-ray shielding testing.

2.1. Material Options

To accomplish the goal of developing a 3D printable material that can be used for in-space habitation on Mars, at least some of the portion of the material must be sourced from Mars because it will not be possible to send all building materials to Mars via cargo missions. Additionally, it will be difficult to justify cargo missions for raw materials only. Therefore, a material solution that uses materials sourced from Mars while reusing shipping materials/packaging materials from other cargo would be ideal. Additionally, since this material is to be used for habitation (building materials that will be used to construct buildings for astronauts to live and work), this material should also provide some radiation protection. Because basalt can be easily mined and produced into fibers on Mars, it makes sense to use basalt fibers to reinforce a thermoplastic material in this application. Several thermoplastics were considered as matrix materials, however, ABS stood out as the most likely to be successful due to low (<240 °C) extrusion temperature, it has already been tested in microgravity experiments, it is recyclable, and could be used as a packaging material for other cargo. Other polymers were considered (see Table 1), but each polymer had some drawbacks.

Table 1. Polymer options for matrix material.

Material Type	Low (< 240 °C) Temperature Extrusion	Has Been 3D Printed in Low Gravity Environments Successfully	Recyclable	Could Be Used in Shipping Materials for Other Cargo
ABS	Yes	Yes [2,47]	Yes [53]	Yes [54]
PLA	Yes	No [2]	Yes [55]	Yes [56]
Nylon	No	Yes [2]	Yes [57]	Yes [56]
HDPE	Yes	Yes [2]	Yes [58]	Yes-common
PC	No	Yes [2]	Yes [59]	Yes-common
PEI-PC	No	Yes [2]	Yes [60]	Potentially

2.2. ABS

ABS is a common 3D printing material and offers several benefits outlined in Table 1. While other materials have an initially higher tensile strength (when no reinforcement is used), it was clear that ABS might still be the best decision due to other factors such as being able to be extruded using lower temperatures, evidence that the material is able to be 3D printed in a microgravity environment, and has been shown that it could be used in packaging materials, then recycled into a building material. The ABS used in this study was naturally colored Sabic MG94 (Filastruder, Snellville, GA, USA). The pellets were dried in a vacuum oven for 24 h at 70 °C to remove any moisture before the material was extruded.

2.3. Basalt Fibers

While commonly included as reinforcement in concrete, basalt fibers are unique to the world of additive manufacturing. Basalt was a material of interest for deep-space additive manufacturing due to its abundance on Mars [61]. Basalt can be found on the surface of Mars, making the refinement and procurement process simpler and less expensive than other stronger alternatives such as carbon fiber, graphene oxide, or carbon nanotubes.

Basalt fiber has a density of 2.65 g/cm³, an ultimate tensile strength of 3300 MPa, and a max elongation of 3.2% [62]. Other attractive properties of basalt fiber are its ultraviolet (UV) immunity, low coefficient of thermal expansion, electrical insulation, higher strength retention in elevated temperatures than other materials (such as E-glass), resistance to aggressive liquids, acids, and alkalis, and recyclability, and potentially most important for this application, radiation shielding [63].

Because basalt is commonly used in cement reinforcement which can use fairly long chopped fibers, commercially available fibers are too large for additive manufacturing purposes. Initial attempts to extrude filament using GlobMarble (Brooklyn, NY, USA) basalt fibers with a length of 12 mm and diameter of 13–19 µm [63], were somewhat successful, however, the resulting extruded material was too stiff to properly spooled. Shorter Dreytek (Rockaway, NJ, USA) unsized basalt fibers [64] were used in this study. These Dreytek fibers were chopped to 3 mm and had a measured diameter range of 15–17 µm (see Figure 1).

2.4. Compounding

The ABS and basalt fibers were measured separately at a prescribed weight ratio, and then combined together in a large container and the mixture was stirred by hand (see Figure 1). A standard test spool of 25% fiber ratio filament contained 200 g of material (i.e., a 200 g spool at 25% fiber ratio contained 150 g of ABS and 50 g of basalt fibers). The ABS and BF mixture was compounded in a Randcastle RCP-0500 (Randcastle, Cedar Grove, NJ, USA) single screw mixing extruder. The resulting material diameter from the Randcastle extruder was too big for 3D printing (approximately 5 mm diameter). The 5 mm filament was then cut into pellet sized pieces using a Hellweg MRS-H granulator (Hellweg Maschinenbau GmbH & Co., Roetgen, Germany). The resulting “pellets” were collected in a

clean bag. In between each material ratio tested, the Randcastle compounding extruder was emptied and the Hellweg granulator was cleaned.



Figure 1. (Left) Dreytek 3 mm basalt fibers, (Right) Basalt fibers and ABS pellets premixed for compounding.

2.5. 3D Printer Filament Extrusion

A custom-built filament extrusion system (shown in Figure 2) was used to manufacture filament for testing in a 3D printer. The extruder barrel is heated by three band heaters, each with their own controllable zones. The single screw has a length of 400 mm and a diameter of 20 mm, resulting in an L/D ratio of 20. The die opening has a diameter of 2.5 mm. The die temperature was set to 200 °C, the metering zone temperature was set to 180 °C, and the melting zone was set to 160 °C. As the filament exited the die, it was cooled and hardened by an array of fans blowing room temperature air across the filament. The hardened filament is measured in a Micro Epsilon OptoControl 2500 (Micro Epsilon, Raleigh, NC, USA) laser diameter scanner as it exited the array of cooling fans. The filament next moves into a system of pulling wheels driven by a stepper motor. After the filament is pulled through the wheels, it is fed into a Filawinder (Filastruder, Snellville, GA, USA) filament spooling system where it is spooled for future testing. To ensure quality control of the filament diameter, the information from the diameter laser scanner is relayed to a microcontroller which then adjusts the speed of the stepper motor in the puller system. Incremental adjustments to the pulling speeds are made until the diameter reaches a steady state of 1.75 mm.

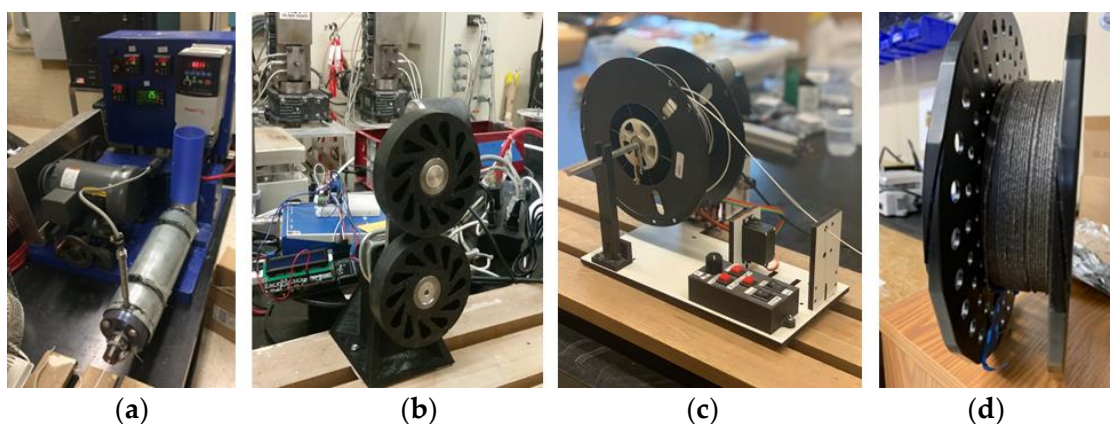


Figure 2. The filament manufacturing extrusion process (a) Single-screw extruder (b) Extrudate puller (c) Spooler (d) Spooled ABS-basalt filament.

Material ratios of 0%, 10%, and 25% were all created relatively easily. Each step of the process functioned well, from initial compounding to material spooling, and finally 3D printing. However, the 40% and 60% ratios proved to have more difficulties. As the fiber content increased, the material became stiffer. At the 40% fiber ratio, the material had become so stiff that it became difficult to spool the material on a standard 3D printer material spool (inner diameter of typical spools is 80–100 mm). A spool with a larger inner diameter (120 mm) was used to spool the 40% fiber ratio.

2.6. 3D Printing

A FlashForge Creator Pro 3D printer (Flashforge USA, Los Angeles, CA, USA) was used to produce all the test samples. The FlashForge Creator Pro and slicer software allow for a range of printing variables to be tested, such as nozzle temperature, build plate temperature, nozzle size, printing toolpath, and extrusion speed. Critical build parameters are shown in Table 2.

Table 2. Critical 3D printing parameters.

Nozzle Temperature (Basalt ratio < 25%)	230 °C
Nozzle Temperature (Basalt ratio > 25%)	250 °C
Building Plate Temperature	110 °C
Nozzle Size	1.0 mm
Layer Height	0.2 mm
Toolpath	+/- 45° alternating with each layer
Number of Outer Perimeters	2
Extrusion Speed	30 mm/s
Build late Material	Glass with ABS slurry (acetone and ABS)

Nozzle temperature was increased to 250 °C from 230 °C when basalt fiber ratios were higher than 25%. With higher ratios of basalt fiber, the viscosity of the composite material decreased and caused nozzle clogging and drive gear filament shredding issues. Changing the extrusion temperature to 250 °C reduced these jamming problems. As with most ABS 3D printing, warping can be an issue for unheated build chambers. To combat this, the build plate was heated to 110 °C, however, this was not enough. The heated glass build plate was also coated with an “ABS slurry”, a common solution to ABS warping issues. ABS slurry is a mixture of approximately 100 mL of acetone with 10–20 g of ABS dissolved in the solution. The ABS slurry sticks firmly to the build plate allowing the first 3D printed layer to also stick firmly and decrease the amount of warping.

2.7. Material Testing

Mechanical properties testing was conducted in accordance to relevant and applicable ASTM standards: ASTM D638 (tensile), ASTM D695 (compression), ASTM D790 (flexural) and ASTM D256 (Izod impact strength). For each ratio tested, at least six samples of each destructive test were printed and tested. For tensile testing and flexural testing, an MTS Insight (MTS, Eden Prairie, MN, USA) electromechanical testing system with a 5 kN load cell and a 20 mm gauge length extensometer was used. For compression testing, an MTS Landmark Universal Testing Machine (MTS, Eden Prairie, MN, USA) was used with a 100 kN load cell and a built-in linear variable differential transformer (LVDT) to measure extension. Impact testing was conducted on a calibrated custom built Izod impact tester.

Optical (Keyence VHX 600 (Keyence Corporation of America, Itasca, IL, USA)) and laser scanning topographic microscopes (Keyence VK-9710 (Keyence Corporation of America)) were used to image material samples. An NSI M5000 (North Star Imaging, Rogers, MN, USA) X-ray imaging system was used to penetrate material samples with X-rays to determine X-ray shielding characteristics and uniform mixing of fibers.

3. Results

3.1. Material Compounding, 1.75 mm Filament Extrusion and 3D Printing

Material with fiber ratios of 0%, 10%, 25%, 40%, and 60% were compounded using Sabic MG94 ABS and Dreytek 3 mm chopped basalt fibers in a Randcastle single screw mixing extruder. Figure 3 shows a cross section of the resulting material. Through the extrusion process, many of the fibers aligned into the extrusion direction. The center (where shear stress is lowest) shows the most fibers out of alignment. Samples of this material were dissolved in acetone, and the fibers were removed from the material. By viewing the fibers under the Keyence VHX 600 microscope, the fibers were determined to have been broken down into smaller lengths, with an average size of 280 μm . This compounded material would later be chopped into 2–3 mm “pellets” to be fed into the filament extruder. This chopping process did not significantly affect the average fiber size, with fibers averaging 271 μm in length after “pelletizing”.

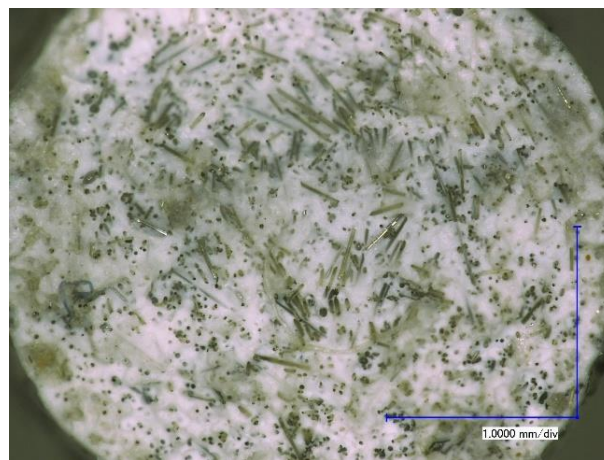


Figure 3. Fiber distribution of 25% fiber ratio compounded material.

The material underwent another extrusion process to turn the compounded pellets into 3D printing filament at 1.75 mm diameter. After this extrusion process, nearly all of the fibers were aligned in the extrusion direction. Figure 4 shows fiber orientation for all four fiber ratios (10%, 25%, 40%, and 60%) at this stage in the process. Light/dark circular spots in the images represent the tops of fibers, or holes where fibers were pulled out of the matrix as the sample was created. Other research has shown [10] that fibers align more through the 3D printing process. Figure 5 shows a cross section of a tensile sample after testing.

Compounding with the Randcastle extruder was easily accomplished for all fiber ratios. Similarly, 1.75 mm filament extrusion was also accomplished for all fiber ratios. However, fiber ratios above 40% were difficult to use in the 3D printer. Difficulties included filament snapping between the spool and the 3D printer extruder when bends are required, nozzle clogging, filament breaking in the drive gear section of the extruder, and significant part warping after printing. The 60% fiber ratio was not able to be spooled with a reasonably sized spool. Attempts were made to hand-feed the 60% fiber ratio filament into the 3D printer in 200 mm lengths of straight pieces. The 3D printing issues found with the 40% fiber ratio material were magnified with the 60% fiber ratio material and no feasible samples were produced. A small example of printed samples is shown in Figure 6, before and after having been tested. Because of the alternating $\pm 45^\circ$ deposition toolpath, fibers can be seen oriented in both directions and layers can be distinguished.

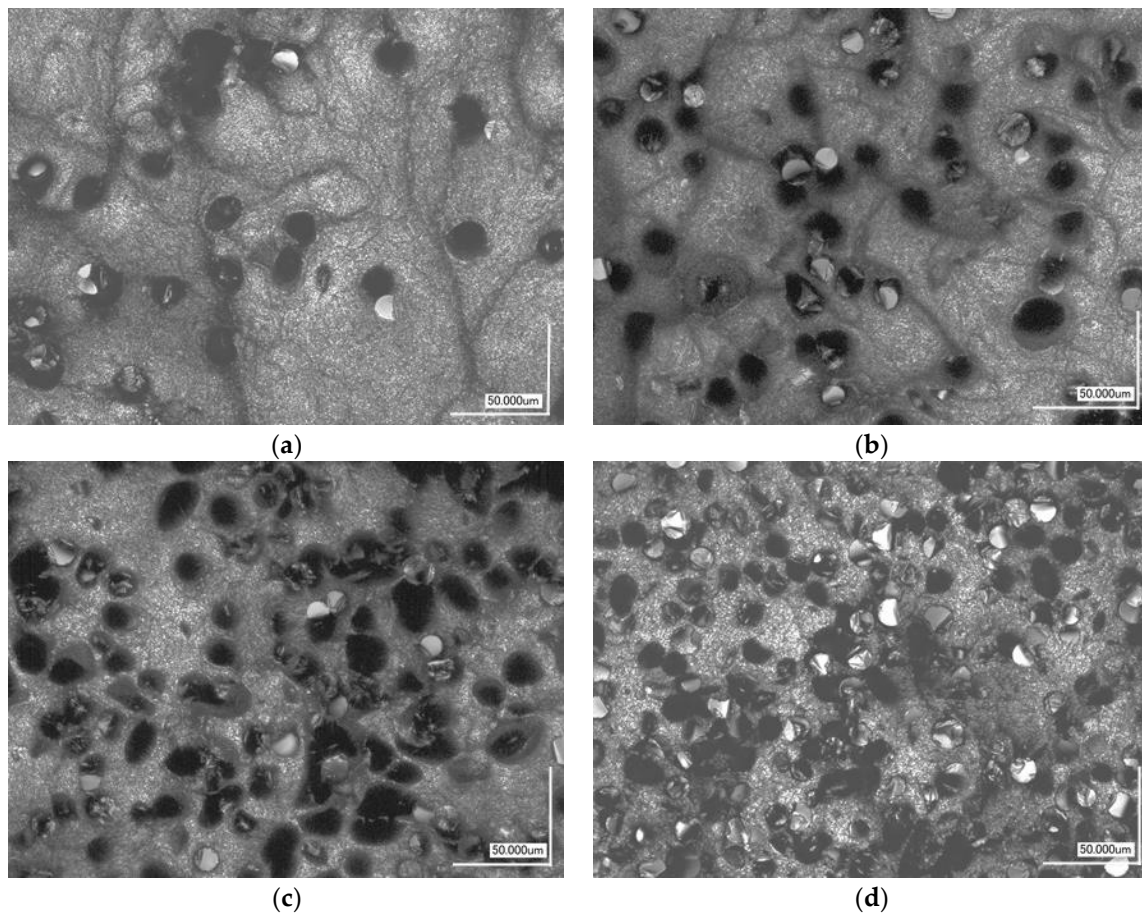


Figure 4. (a) 10% basalt fiber, (b) 25% basalt fiber, (c) 40% basalt fiber, (d) 60% basalt fiber.

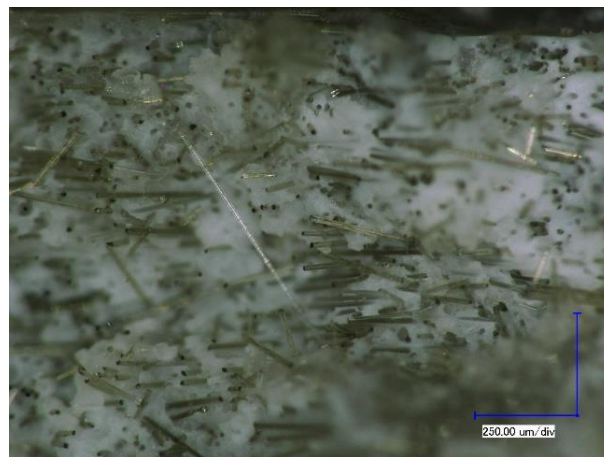


Figure 5. Fiber distribution of the final 3D printed component.

Control samples of 100% ABS (no fiber) were manufactured and tested to compare to commercially available ABS. The ABS filament produced had similar results to commercially available ABS material used in 3D printing (31 MPa tensile strength listed by Stratasys for its ABS-M30 [65])—see results in the next section for full details.

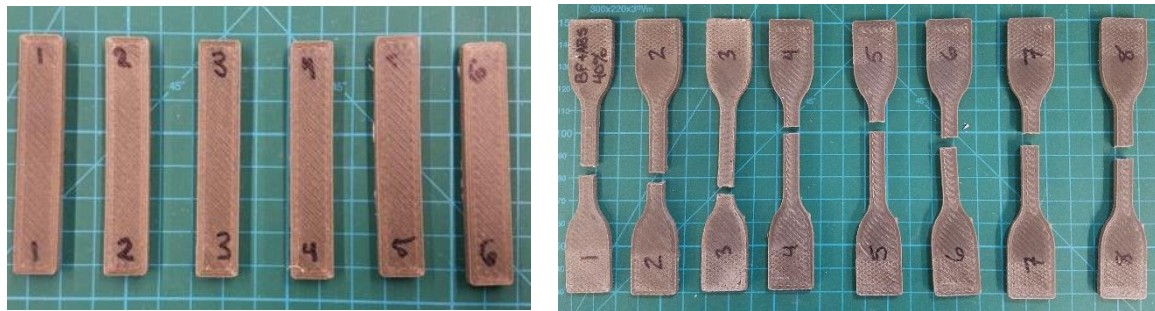


Figure 6. (Left) Examples of 3D printed ABS-Basalt composite material samples (25% fiber content), (Right) Tensile samples after samples had been tested (40% fiber content).

3.2. Material Property Testing Results

3.2.1. Tensile Testing

Table 3 outlines the tensile results of increasing fiber percentage in ABS. Along with Table 3, Figure 7 shows a typical representation of the stress/strain relationship.

Table 3. Tensile Testing Results.

Composite Material Ratio	Tensile Strength (MPa)	Yield Strength (MPa)	Modulus of Elasticity (GPa)	Max Elongation (%)
ABS	36.55 ± 2.51	32.07 ± 3.69	2.15 ± 0.14	9.92 ± 0.97
ABS & 10% BF	45.92 ± 2.06	40.36 ± 1.90	3.66 ± 0.24	2.82 ± 0.43
ABS & 25% BF	50.58 ± 3.42	45.89 ± 3.36	4.56 ± 0.39	1.64 ± 0.50
ABS & 40% BF	45.64 ± 0.64	43.20 ± 1.43	4.79 ± 0.35	1.33 ± 0.24

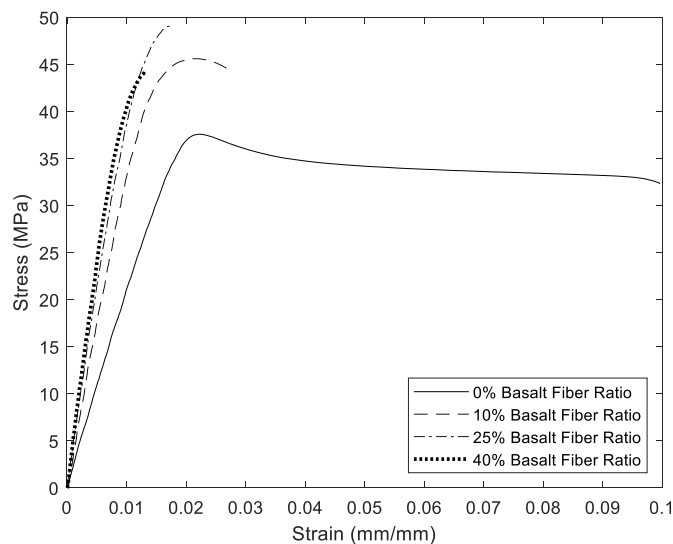


Figure 7. Representative tensile stress/strain results for each fiber ratio.

As was expected, tensile strengths increased with increasing fiber content and maximum elongation decreased with increased fiber content. However, fiber ratios above 25% were not stronger than the 25% fiber ratio, but were stiffer, and maximum elongation also decreased.

3.2.2. Flexural Testing

Flexural testing results in Table 4 were obtained using the MTS Insight tester with a 3-point bending apparatus. The flexural strength and modulus increased with higher concentrations of basalt fiber present in the sample. It should be noted that the 40% fiber ratio samples had defects during the printing stage, likely contributing to the decrease in the ultimate flexural strength and yield strength. As was expected, strengths and flexural modulus increased with increasing fiber content ratio, but the maximum strain decreased due to an increase in stiffness from the presence of fibers. Figure 8 shows representative flexural stress-strain curves for each fiber ratio.

Table 4. Flexural Testing Results.

Composite Material Ratio	Ultimate Flexural Strength (MPa)	Yield Strength (MPa)	Flexural Modulus (GPa)	Max Flexural Strain (%)
ABS	56.94 ± 1.24	46.83 ± 1.53	1.81 ± 0.10	9.72 ± 1.07
ABS & 10% BF	67.30 ± 1.69	51.38 ± 2.12	2.76 ± 0.07	4.71 ± 0.54
ABS & 25% BF	68.51 ± 0.82	62.18 ± 3.87	3.05 ± 0.26	3.72 ± 0.64
ABS & 40% BF	62.05 ± 0.98	49.89 ± 0.54	3.23 ± 0.21	3.21 ± 0.61

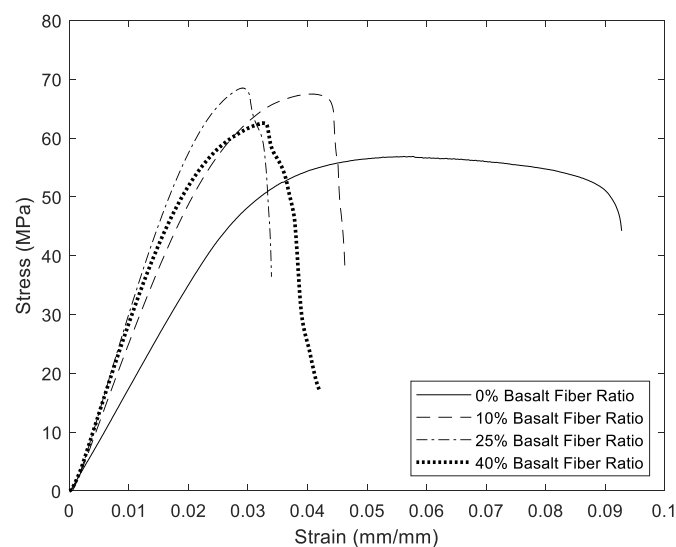


Figure 8. Representative flexural stress/strain results for each fiber ratio.

3.2.3. Compression Testing

3D printed samples of the ABS-Basalt material tested in compression did not exhibit large changes from the control samples, see Table 5 and Figure 9 for full results. Ultimate Compressive Strength did not change significantly, however, a slight increase in compressive modulus of elasticity was observed. The compressive modulus values stayed steady at approximately 1.7 GPa, from 10% to 40% basalt fiber ratio.

Table 5. Compression Testing Results.

Composite Material Ratio	Ultimate Compression Strength (MPa)	Compressive Modulus (GPa)
ABS	54.51 ± 2.50	1.49 ± 0.22
ABS & 10% BF	52.90 ± 1.73	1.67 ± 0.03
ABS & 25% BF	59.38 ± 1.80	1.69 ± 0.20
ABS & 40% BF	56.71 ± 0.72	1.70 ± 0.05

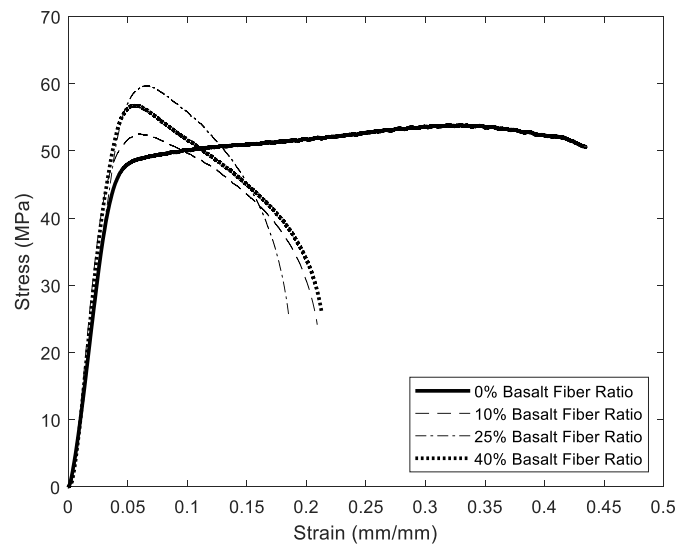


Figure 9. Representative compressive stress/strain results for each fiber ratio.

3.2.4. Izod Impact Testing

Izod impact strength testing was completed to measure the energy absorption of each fiber content ratio—see Table 6 for full results. As expected from theory and from previous tensile and flexural results, increasing fiber content increased the brittleness of the material. Each increase in fiber content led to a decrease in impact energy.

Table 6. Izod Impact Testing Results.

Composite Material Ratio	Impact Energy (J/m)
ABS	277.06 ± 9.67
ABS & 10% BF	60.69 ± 2.68
ABS & 25% BF	53.41 ± 5.06
ABS & 40% BF	41.42 ± 7.32

3.2.5. Digital Radiography

An NSI M500 CT scanner (North Star Imaging) was used to measure the X-ray radiation shielding properties of the resulting materials capable of being 3D printed. Figure 10 shows samples of varying fiber ratios that were X-ray scanned together. In the image, lighter colors mean that more of the X-rays are allowed to pass through the material to reach the detector, darker colors mean more the X-rays have been blocked from being received by the detector. In the case of Figure 10, it is clear by eye that the addition of basalt fibers to the material have increased the number of X-rays that have been shielded from the detector. The amount of X-ray intensity detected by the 14-bit X-ray detector over

a specified time is converted to a color on the screen for visual interpretation. Using Matlab Image Analysis, the colors of the images were quantified—see Table 7.



Figure 10. X-ray image of tensile samples with various basalt composition. From left to right: 0%, 10%, 25%, 40%.

Table 7. Color quantification of X-ray material samples.

Composite Material Ratio	Average Gray Color Scale Value (0 = Pure Black, 255 = Pure White)	% of X-rays Shielded (as Compared to Neat ABS)
ABS	125.61 ± 3.06	0.0%
ABS & 10% BF	85.47 ± 2.63	32.0%
ABS & 25% BF	57.06 ± 1.89	54.6%
ABS & 40% BF	28.55 ± 1.77	77.3%

4. Discussion

The end use of this material leads to a different set of goals and constraints than most traditional composite materials. Because the addition of basalt fibers provides radiation shielding and strength enhancements, the cost is negligible compared to the cost of shipping matrix materials to pair with the fibers, it is advantageous to use as much basalt fiber as can practically be put in the material, while still allowing the filament extrusion and 3D printing deposition process to function as they normally would function.

ABS-Basalt pellets were able to be made for each fiber ratio tested (0%, 10%, 25%, 40%, and 60%). Filament of appropriate diameter (1.75 mm) for 3D printing was also able to be manufactured for each fiber ratio. The 60% fiber ratio proved to be too stiff for spooling and is not a viable solution for small-scale 3D printing. However, large 3D printers sized for full-scale habitats will not use spools of filament. They will be fed by pellets into a pellet extruder. While unable to test 60% fiber ratio material in a small-scale 3D printer, this may still be an option for larger 3D printers with pellet extruders.

In tensile, flexural, and compression testing, mechanical material properties increased (stronger and stiffer) with increasing fiber ratio until reaching the 40% fiber ratio. There are two possible reasons the 40% fiber ratio did not see strength or stiffness increases. As noted in Section 2.6, the extrusion (nozzle) temperature of the 3D printer was increased to 250 °C to allow the material to have a low enough viscosity to extrude from the nozzle at a consistent rate. Heating ABS to high temperatures will eventually cause thermal decomposition [66]. The warmer extrusion nozzle temperature (250 °C) is only 20 °C warmer than standard 3D printing temperature for ABS. Although some decomposition

may have started to occur, this is not thought to be the main source of strength loss. As shown in Figure 4, the fibers are packed tightly in the material cross section and are in some locations making contact with other fibers. This likely is not promoting good bonding between the fiber and the matrix material, leaving small stress concentrators inside the material, causing premature failure.

Tables 3–6 show increases in strength and stiffness. By adding 25% (by weight) basalt fiber to ABS, tensile strength improved nearly 40%, increasing from 36.55 MPa to 50.58 MPa, while Modulus of Elasticity increased about 120% from 2.15 GPa to 4.79 GPa. Flexural strength increased by about 20% from 56.94 MPa to 68.51 MPa, while Flexural Modulus increased by about 70% from 1.81 GPa to 3.05 GPa. While compression results did not see much strength improvements, the addition of fibers also did not decrease compressive strength. This is important when considering that basalt fibers provide radiation shielding.

Figure 10 shows digital radiographs of samples 3D printed and penetrated with X-rays. Because the colors of each sample are relatively constant across the sample, the images show that fibers are evenly distributed throughout the sample. Earlier attempts to use other methods to mix basalt fibers and ABS matrix material did not produce an evenly mixed composite material. Figure 10 and Table 7 also clearly show that the material is providing X-ray radiation shielding protection. However, the surface of Mars is exposed to higher energy radiation (higher than X-rays) and the basalt fibers may not provide the same level of shielding to other types of space radiation as it does to X-ray radiation.

As one last test to determine the validity of using this material for 3D printing applications, several real-world objects were produced. In Figure 11, three of these objects are shown: an open-faced 12 mm wrench, a helical gear, and a handrail clamp. Similar objects were printed as test objects in the original 3D printing in microgravity experiments at the ISS [47]. While none of these objects were tested to failure, the objects were much stiffer than their control ABS counterparts.

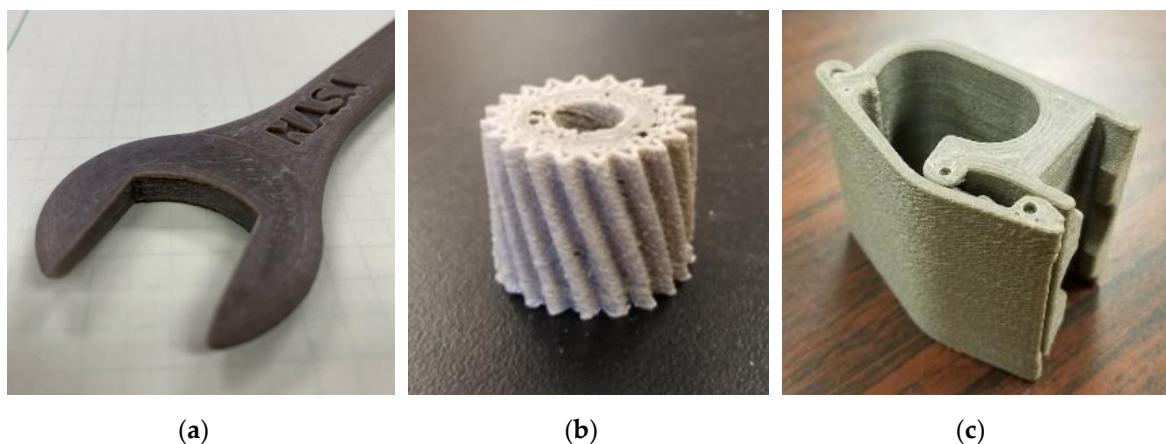


Figure 11. (a) 12 mm wrench (25% fiber), (b) Helical gear (10% fiber), (c) Handrail Clamp (25% fiber).

5. Conclusions

Basalt fiber reinforced ABS filament was produced at five different fiber ratios and used to 3D print samples for testing. Mechanical testing showed that strengths and stiffness improved until 40% fiber ratio, at which point stiffness still increased slightly, but strength was reduced. The most likely reason strengths decreased was due to the tighter packing of fibers in the matrix, which reduced overall quality of bonding between the fiber and the ABS matrix. Digital radiography revealed that the composite material was evenly mixed during the extrusion and deposition processes. X-ray images also showed that the higher the fiber content ratio, the more X-rays were shielded by the material. Also, it was demonstrated that this material could be 3D printed into small useful items, such as wrenches, gears, and clamps.

Further testing needs to be done on this material to learn about its fatigue strength (SN curve). Repeating similar testing to this paper, but adding additional fiber content ratios between 25% and

40% would also be beneficial to future designers. Fiber ratios above 40% should also be tested on large scale 3D printers equipped with a pellet extruder. Finally, studies should be conducted related to the recyclability of ABS packaging materials then used as an ABS-Basalt construction material for 3D printing.

Author Contributions: Material processing and sample manufacturing—B.D., E.S., T.W., A.W., and T.L.; Mechanical Testing—N.C., B.D., M.F., E.S., and T.L.

Funding: This research was funded by the NASA X-Hab Academic Innovation Challenge.

Acknowledgments: The authors would like to thank Christopher Roberts, Kristin Morgan and the rest of the in-space manufacturing team at NASA.

Conflicts of Interest: The authors declare no conflict of interest.

References

- Salotti, J.M.; Heidmann, R. Roadmap to a human Mars mission. *Acta Astronaut.* **2014**, *104*, 558–564. [CrossRef]
- Additive Manufacturing Facility (AMF) User Guide. Made In Space. Available online: <https://static1.squarespace.com/static/56d9b0528259b560ad38cde1/t/58d2dfda3a0411eedc691ad4/1490214884324/AMF+user+guide.pdf> (accessed on 29 April 2016).
- Linck, E.; Crane, K.W.; Zuckerman, B.L.; Corbin, B.A.; Myers, R.M.; Williams, S.R.; Lal, B. Evaluation of a Human Mission to Mars by 2033. 2019. Available online: <https://www.ida.org/-/media/feature/publications/ev/evaluation-of-a-human-mission-to-mars-by-2033/d-10510.ashx> (accessed on 4 September 2019).
- Koch, C.; Hulle, L.V.; Rudolph, N. Investigation of mechanical anisotropy of the fused filament fabrication process via customized tool path generation. *Addit. Manuf.* **2017**, *16*, 138–145. [CrossRef]
- Letcher, T.; Waytashek, M. Material Property Testing of 3D-Printed Specimen in PLA on an Entry-Level 3D Printer. In Proceedings of the ASME IMECE 2014, Montreal, QC, Canada, 14–20 November 2014; Volume 2A. Advanced Manufacturing.
- Ferrell, W.H.; Termaath, S.C. Print Parameter Effects on the Fracture Properties of Fiber Reinforced ABS Composites Fabricated Through Fused Deposition Modeling. In Proceedings of the AIAA Scitech 2019 Forum, San Diego, CA, USA, 7–11 January 2019.
- Rankouhi, B.; Javadpour, S.; Delfanian, F.; Letcher, T. Failure Analysis and Mechanical Characterization of 3D Printed ABS With Respect to Layer Thickness and Orientation. *J. Fail. Anal. Prev.* **2016**, *16*, 467–481. [CrossRef]
- Rahman, K.M.; Letcher, T.; Reese, R. Mechanical Properties of Additively Manufactured PEEK Components Using Fused Filament Fabrication. In Proceedings of the ASME IMECE 2015, Houston, TX, USA, 13–19 November 2015; Volume 2A. Advanced Manufacturing.
- Popescu, D.; Zapciu, A.; Amza, C.; Baciu, F.; Marinescu, R. FDM process parameters influence over the mechanical properties of polymer specimens: A review. *Polym. Test.* **2018**, *69*, 157–166. [CrossRef]
- Compton, B.G.; Lewis, J.A. 3D-Printing of Lightweight Cellular Composites. *Adv. Mater.* **2014**, *26*, 5930–5935. [CrossRef]
- Wei, X.; Li, D.; Jiang, W.; Gu, Z.; Wang, X.; Zhang, Z.; Sun, Z. 3D Printable Graphene Composite. *Sci. Rep.* **2015**, *5*, 11181. [CrossRef]
- Chen, Q.; Mangadlao, J.D.; Wallat, J.; Leon, A.D.; Pokorski, J.K.; Advincula, R.C. 3D Printing Biocompatible Polyurethane/Poly(lactic acid)/Graphene Oxide Nanocomposites: Anisotropic Properties. *ACS Appl. Mater. Interfaces* **2017**, *9*, 4015–4023. [CrossRef]
- Cholleti, E.R.; Gibson, I. ABS Nano Composite Materials in Additive Manufacturing. *IOP Conf. Ser. Mater. Sci. Eng.* **2018**, *455*, 012038. [CrossRef]
- Quill, T.J.; Smith, M.K.; Zhou, T.; Baioumy, M.G.S.; Berenguer, J.P.; Cola, B.A.; Kalaitzidou, K.; Bougher, T.L. Thermal and mechanical properties of 3D printed boron nitride–ABS composites. *Appl. Compos. Mater.* **2017**, *25*, 1205–1217. [CrossRef]
- Parandoush, P.; Lin, D. A review on additive manufacturing of polymer-fiber composites. *Compos. Struct.* **2017**, *182*, 36–53. [CrossRef]
- Ning, F.; Cong, W.; Qiu, J.; Wei, J.; Wang, S. Additive manufacturing of carbon fiber reinforced thermoplastic composites using fused deposition modeling. *Compos. Part B Eng.* **2015**, *80*, 369–378. [CrossRef]

17. Blok, L.G.; Longana, M.L.; Yu, H.; Woods, B.K. Woods, An investigation into 3D printing of fibre reinforced thermoplastic composites. *Addit. Manuf.* **2018**, *22*, 176–186. [[CrossRef](#)]
18. Panda, B.; Paul, S.C.; Tan, M.J. Anisotropic mechanical performance of 3D printed fiber reinforced sustainable construction material. *Mater. Lett.* **2017**, *209*, 146–149. [[CrossRef](#)]
19. Hofstätter, T.; Pedersen, D.B.; Tosello, G.; Hansen, H.N. Applications of Fiber-Reinforced Polymers in Additive Manufacturing. *Proced. CIRP* **2017**, *66*, 312–316. [[CrossRef](#)]
20. Türk, D.-A.; Brenni, F.; Zogg, M.; Meboldt, M. Mechanical characterization of 3D printed polymers for fiber reinforced polymers processing. *Mater. Des.* **2017**, *118*, 256–265. [[CrossRef](#)]
21. Sauer, M.J. Evaluation of the Mechanical Properties of 3D Printed Carbon Fiber Composites. Ph.D. Thesis, South Dakota State University, Brookings, SD, USA, 2018.
22. Yang, C.; Tian, X.; Liu, T.; Cao, Y.; Li, D. 3D printing for continuous fiber reinforced thermoplastic composites: Mechanism and performance. *Rapid Prototyp. J.* **2017**, *23*, 209–215. [[CrossRef](#)]
23. Nakagawa, Y.; Mori K-i Maeno, T. 3D printing of carbon fibre-reinforced plastic parts. *Int. J. Adv. Manuf. Technol.* **2017**, *91*, 2811–2817. [[CrossRef](#)]
24. Melenka, G.W.; Cheung, B.K.O.; Schofield, J.S.; Dawson, M.R.; Carey, J.P. Evaluation and prediction of the tensile properties of continuous fiber-reinforced 3D printed structures. *Compos. Struct.* **2016**, *153*, 866–875. [[CrossRef](#)]
25. Christensen, P.R.; Bandfield, J.L.; Bell, J.F., III; Gorelick, N.; Hamilton, V.E.; Ivanov, A.; Jakosky, B.M.; Kieffer, H.H.; Lane, M.D.; et al. Morphology and Composition of the Surface of Mars: Mars Odyssey THEMIS Results. *Science* **2003**, *300*, 2056–2061. [[CrossRef](#)]
26. Christensen, P.R.; Bandfield, J.L.; Smith, M.D.; Hamilton, V.E.; Clark, R.N. Identification of a basaltic component on the Martian surface from Thermal Emission Spectrometer data. *J. Geophys. Res. Planets* **2000**, *105*, 9609–9621. [[CrossRef](#)]
27. Sharp, T. What is Mars Made Of? Composition of Planet Mars. 12 December 2017. Available online: <https://www.space.com/16895-what-is-mars-made-of.html> (accessed on 4 September 2019).
28. Mahltig, B. Basalt Fibers. In *Inorganic and Composite Fibers*; Elsevier: Amsterdam, The Netherlands, 2018; pp. 195–217.
29. Fiore, V.; Scalici, T.; Di Bella, G.; Valenza, A. A review on basalt fibre and its composites. *Compos. Part B Eng.* **2015**, *74*, 74–94. [[CrossRef](#)]
30. Dhand, V.; Mittal, G.; Rhee, K.Y.; Park, S.-J.; Hui, D. A short review on basalt fiber reinforced polymer composites. *Compos. Part B Eng.* **2015**, *73*, 166–180. [[CrossRef](#)]
31. Czigány, T. Discontinuous Basalt Fiber-Reinforced Hybrid Composites. In *Polymer Composites*; Springer: Berlin, Germany, 2005; pp. 309–328.
32. Czigány, T. Basalt Fiber Reinforced Hybrid Polymer Composites. *Mater. Sci. Forum* **2005**, *473*, 59–66. [[CrossRef](#)]
33. Deák, T.; Czigány, T.; Maršáľková, M.; Militký, J. Manufacturing and testing of long basalt fiber reinforced thermoplastic matrix composites. *Polym. Eng. Sci.* **2010**, *12*, 2448–2456. [[CrossRef](#)]
34. Lopresto, V.; Leone, C.; De Iorio, I. Mechanical characterisation of basalt fibre reinforced plastic. *Compos. Part B Eng.* **2011**, *42*, 717–723. [[CrossRef](#)]
35. Colombo, C.; Vergani, L.; Burman, M. Static and fatigue characterisation of new basalt fibre reinforced composites. *Compos. Struct.* **2012**, *94*, 1165–1174. [[CrossRef](#)]
36. Liu, S.; Wu, G.; Yu, J.; Chen, X.; Guo, J.; Zhang, X.; Wang, P.; Yin, X. Surface modification of basalt fiber (BF) for improving compatibilities between BF and poly lactic acid (PLA) matrix. *Compos. Interfaces* **2019**, *26*, 275–290. [[CrossRef](#)]
37. Sang, L.; Han, S.; Peng, X.; Jian, X.; Wang, J. Development of 3D-printed basalt fiber reinforced thermoplastic honeycombs with enhanced compressive mechanical properties. *Compos. Part A Appl. Sci. Manuf.* **2019**, *125*, 105518. [[CrossRef](#)]
38. Sang, L.; Han, S.; Peng, X.; Jian, X.; Wang, J. Development of short basalt fiber reinforced polylactide composites and their feasible evaluation for 3D printing applications. *Compos. Part B Eng.* **2019**, *164*, 629–639. [[CrossRef](#)]
39. Yu, S.; Hwang, Y.H.; Hwang, J.Y.; Hong, S.H. Analytical study on the 3D-printed structure and mechanical properties of basalt fiber-reinforced PLA composites using X-ray microscopy. *Compos. Sci. Technol.* **2019**, *175*, 18–27. [[CrossRef](#)]

40. Wong, J.Y. 3D Printing Applications for Space Missions. *Aerosp. Med. Hum. Perform.* **2016**, *87*, 580–582. [[CrossRef](#)]
41. Wong, J.Y.; Pfahnl, A.C. 3D Printing of Surgical Instruments for Long-Duration Space Missions. *Aviat. Sp. Environ. Med.* **2014**, *85*, 758–763. [[CrossRef](#)]
42. Muir, M.; Haddud, A. Additive manufacturing in the mechanical engineering and medical industries spare parts supply chain. *J. Manuf. Technol. Manag.* **2017**, *29*, 372–397. [[CrossRef](#)]
43. Dordlofva, C.; Lindwall, A.; Törlind, P. Opportunities and Challenges for Additive Manufacturing in space applications. In Proceedings of the NordDesign 2016, Trondheim, Norway, 10–12 August 2016; Volume 1.
44. Prater, T.; Werkheiser, N.; Ledbetter, F.; Timucin, D.; Wheeler, K.; Snyder, M. 3D Printing in Zero G Technology Demonstration Mission: complete experimental results and summary of related material modeling efforts. *Int. J. Adv. Manuf. Technol.* **2019**, *101*, 391. [[CrossRef](#)]
45. Rankouhi, B.; Javadvpour, S.; Delfanian, F.; McTaggart, R.; Letcher, T. Experimental Investigation of Mechanical Performance and Printability of Gamma-Irradiated Additively Manufactured ABS. *J. Mater. Eng. Perform.* **2018**, *27*, 3643–3654. [[CrossRef](#)]
46. Thomas, D.; Snyder, M.P.; Napoli, M.; Joyce, E.R.; Shestopole, P.; Letcher, T. Effect of Acrylonitrile Butadiene Styrene Melt Extrusion Additive Manufacturing on Mechanical Performance in Reduced Gravity. In Proceedings of the AIAA SPACE and Astronautics Forum and Exposition, Orlando, FL, USA, 12–14 September 2017.
47. Prater, T.J.; Werkheiser, N.J.; Ledbetter, F.E., III. *Summary Report on Phase I Results from the 3D Printing in Zero G Technology Demonstration Mission*; 2016; NASA/TP-2018-219855/Vol 2, M-1457 Technical Report; Volume 1. Available online: <https://ntrs.nasa.gov/archive/nasa/casi.ntrs.nasa.gov/20160008972.pdf> (accessed on 4 September 2019).
48. Goulas, A.; Binner, J.G.; Harris, R.A.; Friel, R.J. Assessing extraterrestrial regolith material simulants for in-situ resource utilisation based 3D printing. *Appl. Mater. Today* **2017**, *6*, 54–61. [[CrossRef](#)]
49. Cesaretti, G.; Dini, E.; Kestelier, X.D.; Colla, V.; Pambaguian, L. Building components for an outpost on the Lunar soil by means of a novel 3D printing technology. *Acta Astronaut.* **2014**, *93*, 430–450. [[CrossRef](#)]
50. Lim, S.; Prabhu, V.L.; Anand, M.; Taylor, L.A. Extra-terrestrial construction processes—Advancements, opportunities and challenges. *Adv. Space Res.* **2017**, *60*, 1413–1429. [[CrossRef](#)]
51. Meurisse, A.; Makaya, A.; Willsch, C.; Sperl, M. Solar 3D printing of lunar regolith. *Acta Astronaut.* **2018**, *152*, 800–810. [[CrossRef](#)]
52. Kading, B.; Straub, J. Utilizing in-situ resources and 3D printing structures for a manned Mars mission. *Acta Astronaut.* **2015**, *107*, 317–326. [[CrossRef](#)]
53. Cushing, J.; Freedman, M.; Turner, K.; Muhlbauer, R.L.; Levedahl, B.; Slostad, J.; Hoyt, R.P.; Kim, T.; Werkheiser, M.J. Building a sustainable in-space manufacturing ecosystem: Positrusion and crissp. In Proceedings of the AIAA SPACE 2016, Long Beach, CA, USA, 13–16 September 2016; p. 5396.
54. Oswald, L.M.; McClanahan, J.D.; Cato, O.; GREASE, Co. McClanahan. Bulk Shipping Container. U.S. Patent No. 4,165,024, 21 August 1979.
55. Tian, X.; Liu, T.; Wang, Q.; Dilmurat, A.; Li, D.; Ziegmann, G. Recycling and remanufacturing of 3D printed continuous carbon fiber reinforced PLA composites. *J. Clean. Product.* **2017**, *142*, 1609–1618. [[CrossRef](#)]
56. Raheem, D. Application of plastics and paper as food packaging materials—an overview. *Emir. J. Food Agric.* **2017**, *25*, 177–188. [[CrossRef](#)]
57. Lozano-González, M.J.; Rodriguez-Hernandez, M.T.; Gonzalez-De Los Santos, E.A.; Villalpando-Olmos, J. Physical–mechanical properties and morphological study on nylon-6 recycling by injection molding. *J. Appl. Polym. Sci.* **2000**, *76*, 851–858. [[CrossRef](#)]
58. Chong, S.; Pan, G.T.; Khalid, M.; Yang, T.C.K.; Hung, S.T.; Huang, C.M. Physical characterization and pre-assessment of recycled high-density polyethylene as 3D printing material. *J. Polym. Environ.* **2017**, *25*, 136–145. [[CrossRef](#)]
59. Antonakou, E.V.; Achilias, D.S. Recent advances in polycarbonate recycling: A review of degradation methods and their mechanisms. *Waste Biomass Valoriz.* **2013**, *4*, 9–21. [[CrossRef](#)]
60. Prater, T.; Werkheiser, M.J.; Ledbetter, F.; Morgan, K. In-Space Manufacturing at NASA Marshall Space Flight Center: A Portfolio of Fabrication and Recycling Technology Development for the International Space Station. In Proceedings of the 2018 AIAA SPACE and Astronautics Forum and Exposition, Orlando, FL, USA, 17–18 September 2018.

61. Rocks on Mars: Basalt, Shale, Sandstone. Conglomerate *Geology.com*. 2015. Available online: <https://geology.com/stories/13/rocks-on-mars/> (accessed on 4 September 2019).
62. He, J.; Shi, J.; Cao, X.; Hu, Y. Tensile Mechanical Properties and Failure Modes of a Basalt Fiber/Epoxy Resin Composite Material. *Adv. Civ. Eng.* **2018**, *2018*, 1–10. [CrossRef]
63. GlobMarble. GlobMarble. 2016. Available online: <https://globmarble.com/basalt-chopped-fibers-for-polymers-concrete.html> (accessed on 4 September 2019).
64. Super Thin Basalt Fiber Technical Data Sheet. 24 April 2015. Available online: <https://www.dreytek.com/wp-content/uploads/2016/09/Micro-Basalt-Faser-englisch-01--e1476264928963.jpg> (accessed on 4 September 2019).
65. ABS-M30: A High Strength 3D Printing Material|Stratasys. Stratasys. 2019. Available online: <https://www.stratasys.com/materials/search/abs-m30> (accessed on 4 September 2019).
66. Thermal Decomposition Measurement of ABS resin I. Available online: https://www.hitachihightech.com/file/global/pdf/products/science/appli/ana/thermal/application_TA_066e.pdf (accessed on 4 September 2019).



© 2019 by the authors. Licensee MDPI, Basel, Switzerland. This article is an open access article distributed under the terms and conditions of the Creative Commons Attribution (CC BY) license (<http://creativecommons.org/licenses/by/4.0/>).